Modulation Recognition of Digital Signal Based on Decision Tree and Support Vector Machine

Fugang Liu(✉), Ziwei Zhang, Shuang Zheng, and Zhaoju Jia

Heilongjiang University of Science and Technology, Harbin 150022, China
liufugang_36@163.com

Abstract. The modulation recognition of digital signal is widely used in the field of communication. In this paper, a decision tree modulation recognition algorithm based on feature extraction and a conventional classifier recognition based on SVM are proposed. 9 kinds of common digital signals are identified and simulated. The results show that the recognition rate of SVM classifier and decision tree is high at low SNR.

Keywords: Modulation recognition · Feature extraction · SVM

1 Introduction

Modulation recognition and classification of wireless communication signals is vital when the electromagnetic spectrum is shared among civilian, government, and military to improve spectrum efficiency and shortage problem. Fast recognition and classification of a wireless signal is a significant process for accurately learning and reliably sharing the spectrum to improve spectrum utilization efficiency [1].

Early modulation parameters were mainly identified by using some external instruments and the experience of artificial individuals. This method of manual analysis and judgment is inefficient, expensive and its accuracy is not guaranteed. With the development of science and technology, modulation recognition technology has been rapidly improved, and automatic modulation recognition (AMR) technology has emerged. As shown in Fig. 1, one of AMR algorithms is maximum likelihood hypothesis recognition method based on Bayesian decision theory. There are some common algorithms such as Average likelihood ratio rest (ALRT) [2–4], Generalized Likelihood Ratio Test (GLRT) [5], Hybrid LRT [6, 7], Quasi-Hybrid LRT [8, 9] and some improved algorithms [10–13]. Maximum likelihood algorithm can achieve optimal recognition performance theoretically by minimizing the probability of misjudgment. This method can ideally obtain high recognition rate by using short message. However, the algorithm requires more prior knowledge (such as carrier rate, channel response information, signal and noise power) and huge computation, which is not conducive to the application of recognition technology.

X. Jiang and P. Li (Eds.): GreeNets 2020, LNICST 333, pp. 140–150, 2020.
https://doi.org/10.1007/978-3-030-62483-5_15

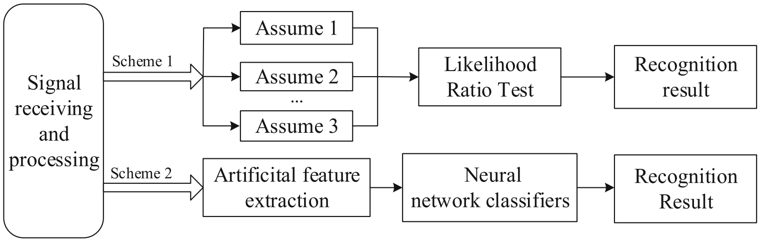

Fig. 1. Two AMR schemes

The scheme 2 in Fig. 1 is based on feature extraction. It has received increasing interest for its application in spectrum sensing and modulation recognition. In this scheme, there is no threshold setting, and the computation is less than likelihood ratio test scheme.

The modulation recognition technique based on feature extraction can be divided into three steps: signal preprocessing, feature extraction and classification (recognition).

(1) Signal preprocessing: This step mainly completes the necessary pre-processing of received signal data. It includes carrier synchronization, frequency down conversion, noise suppression, estimation and processing of parameters such as signal-to-noise ratio, symbol period and carrier frequency.
(2) Feature extraction: According to different schemes, this step can be divided into two categories: manual feature extraction and automatic feature extraction. The main task is to use signal processing tools such as wavelet, cyclostationary and cumulant to extract the characteristic parameters of signal in time domain, frequency domain or the other transform domain.
(3) Classification and recognition: Different algorithms correspond to different classifiers. According to the extracted feature parameters and classification requirements, the applicable decision rules and recognition classifiers are selected and determined.

The accuracy of feature data has a great impact on the performance of learning algorithm and recognition results. Reviewing the literature in recent years, these algorithms for modulation recognition mainly include decision tree, the k-nearest neighbor[14], support vector machine [15], artificial neural network and some hybrid algorithms [16].

In this paper, we study the recent research work and study the modulation recognition method based on feature extraction. We focus on two methods: decision tree method and support vector machine method. In this paper, the feature parameters of MPSK, MFSK, MASK and MQAM are extracted from the features of high-order cumulant, instantaneous and wavelet transform. Then, the modulation recognition of communication signals is carried out by using decision tree and support vector machine respectively. Finally, the simulation experiment is carried out.

2 Decision Tree and Support Vector Machine

Decision Tree is a decision analysis method, which is a graphical method to evaluate project risk and judge the feasibility of net present value by constructing a Decision

Tree to obtain the probability that the expected value of net present value is greater than or equal to zero on the basis of knowing the probability of various situations. Because this kind of decision branch is drawn like the trunk of a tree, it is called decision tree. In machine learning, decision tree is a predictive model, which represents a mapping relationship between object properties and object values.

In SVM regression, the input samples are not linear in general, we need to use a non-linear relationship to map each input sample into a high-dimensional feature space, to make it as linear as possible in the high-dimensional space. This makes it easier for us to use linear relations to deal with them, and then to get the Nonlinear regression of the source space of the sample.

The regression function is

$$f(x, w) = w\psi(x) + b = (w, \psi(x)) + b \tag{1}$$

w is the weight vector and b is a constant. The SVM regression problem is generally solved by introducing a loss function. Coefficients w and b in equation.

The minimization of is estimated by:

$$\min Q = \frac{1}{2}\|w\|^2 + C\sum_{i=1}^{m}(\xi_i^{'} + \xi_i) \tag{2}$$

The constraints are:

$$\begin{cases} wx_i + b - y_i \le \varepsilon + \xi_i \\ y_i - wx_i - b \le \varepsilon + \xi_i^{'} \\ \varepsilon, \xi_i^{'} \ge 0; i = 1, \ldots\ldots m \end{cases} \tag{3}$$

Where C is the error penalty factor, ξ_i and $\xi_i^{'}$ relaxation factors, and ε is the loss function.

Since the feature space has a high dimension and the objective function is not differentiable, the Lagrangian multiplier method is used to calculate the feature space.

Quadratic programming problems with linear inequality constraints:

$$W(a_i, b_i) = \sum_{i=1}^{m} y_i(a_i - b_i) - \varepsilon\sum_{i=1}^{m}(a_i + a_i^{'}) - \frac{1}{2}\sum_{i,j=1}^{m}(a_i - a_i^{'})(a_j - a_i^{'})x_i x_j^{'} \tag{4}$$

The constraints are:

$$\begin{cases} \sum_{i=1}^{m}(a_i - a_i^{\prime}) = 0 \\ a_i \ge 0, a_i \le C \end{cases} \quad i = 1, 2, \ldots.., m \tag{5}$$

$x_i, x_j^{\prime}$ is the input, y_i is the output, a_i and b_i are Lagrangian multipliers. Penalty Factor C is used to control the complexity of regression model and the precision of regression estimation. The larger the C is, the better the fitting degree of the data, that is, the higher the accuracy of the regression estimation, but not unlimitedly large, which may make the model can‘t predict normally, and also used to control the accuracy of the regression estimation, but also control the generalization ability of the model.

3 Feature Parameter Analysis and Extraction of Signal

3.1 Features of Higher Order Cumulants

Because the noise and signal are independent each other, the cumulative amount of Gaussian noise at the fourth order and above is zero according to the nature of high-order accumulation, the effect of Gaussian noise can be ignored. Therefore, the high-order accumulation has a strong noise suppression ability. If the signal received by the receiver has been Carrier synchronization, code element timing, matching filtering, channel noise is Gaussian white noise, then the sequence of code element synchronous sampling and complex signals obtained at the output is:

$$\sum_k a_k \sqrt{E} p(t - kT_s) \exp(\mathrm{j}\theta_c) + n(t) \tag{6}$$

Where, k is 1,2,3, …, N; N is the length of the send element sequence, a_k represents the code element sequence, $p(t)$ is the sender element waveform, the T_s is the code element width, the fc is the carrier frequency, the θ_c is the carrier phase, The E in the energy of the signal, $n(t)$ is the compound white noise with a zero with a zero mean. For the smooth random process $x(t)$ of the zero mean, its P-level mixing moment is defined as:

$$M_{pq} = E\{X(K)^{p-q}\left[X*(K)\right]^q\} \tag{7}$$

The second-order cumulant is:

$$C_{20} = Cum(X, X) = M_{20} \tag{8}$$

$$C_{21} = Cum\left(X, X^*\right) = M_{21} \tag{9}$$

The fourth-order cumulant is:

$$C_{40} = Cum(X, X, X, X) = M_{40} - 3M_{20}^2 \tag{10}$$

$$C_{41} = Cum\left(X, X, X, X^*\right) = M_{41} - 3M_{20}M_{21} \tag{11}$$

$$C_{42} = Cum\left(X, X, X^*, X^*\right) = M_{42} - |M_{20}|^2 - 2M_{21}^2 \tag{12}$$

The sixth-order cumulant is:

$$C_{60} = Cum(X, X, X, X, X, X) = M_{60} - 15M_{40}M_{20} + 30M_{21}^3$$

$$C_{63} = Cum\left(X, X, X, X^*, X^*, X^*\right) = M_{63} - 9M_{42}M_{21} + 9|M_{20}|^2M_{21} + 12M_{21}^3 \tag{14}$$

The three feature parameters extracted based on higher-order cumulants are F_1,F_2 and F_3:

$$F_1 = |C_{40}|/C_{42}, \quad F_2 = |C_{41}|/C_{42}, \quad F_3 = |C_{63}|^2/|C_{42}|^3 \tag{15}$$

As can be seen from Fig. 2, The three features of higher-order cumulants have better performance Robustness at low SNR. F_1 can be used to divide the nine signals into {8PSK, 2FSK, 4FSK} and {2ASK, 2PSK, 16QAM, 64QAM, 4ASK and 4PSK}, {2ASK, 2PSK, 16QAM, 64QAM, 4ASK, 4PSK} can be further divided into {2ASK, 2PSK, 4PSK} and {16QAM, 64QAM, 4ASK} by F_2. Finally, {2ASK, 2PSK, 4PSK} and {16QAM, 64QAM, 4ASK} can be divided into {2ASK, 2PSK} and 4ASK, {16QAM, 64QAM}and 4PSK by F_3. In other words, 4ASK and 4PSK can be recognized by extracting high-order cumulant feature parameters and setting appropriate threshold, and the remaining signals can be divided into three sets: {2ASK, 2PSK}, {16QAM, 64QAM} and {8PSK, 2FSK, 4FSK}.

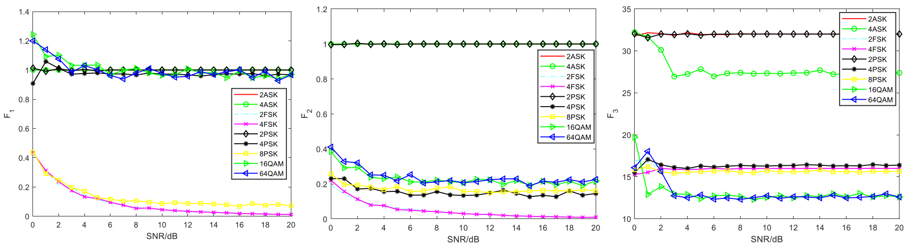

Fig. 2. Specific parameter for F_1, F_2, F_3

3.2 Transient Characteristics

For the real signal $x(t)$, if we do the David Hilbert transform on $x(t)$, then the David Hilbert transform signal is $y(t)$ where the David Hilbert transform formula is:

$$y(t) = \frac{1}{\pi t} \otimes x(t) = \frac{1}{\pi} \int_{-\infty}^{+\infty} \frac{x(\tau)}{t-\tau} d\tau \tag{16}$$

$$s(t) = x(t) + \mathrm{j}y(t) \tag{17}$$

The instantaneous amplitude is

$$A(i) = \left(x^2(i) + y^2(i)\right)^{\frac{1}{2}} \tag{18}$$

The instantaneous phase is

$$\varnothing(i) = \varnothing(i) + C(i) \tag{19}$$

Because $\theta(i)$ has phase collapse, it is modified by Modulo 2

$$C(i) \begin{cases} C(i-1) - 2\pi, \theta(i+1) - \theta(i+1) > \pi \\ C(i-1) + 2\pi, \theta(i) - \theta(i+1) > \pi \\ C(i-1), \text{else} \end{cases} \tag{20}$$

$$\theta(i) = \begin{cases} \tan^{-1}\left[y(i)/x(i)\right],\ x(i) > 0 \\ \tan^{-1}\left[y(i)/x(i)\right] - \pi,\ x(i) < 0, y(i) \geq 0 \\ \tan^{-1}\left[y(i)/x(i)\right] + \pi,\ x(i) < 0, y(i) \geq 0 \\ \pi/2,\ x(i) = 0, y(i) \leq 0 \\ -\pi/2,\ x(i) = 0, y(i) > 0 \end{cases} \tag{21}$$

The instantaneous frequency is

$$f(t) = \frac{1}{2\pi T}[\varnothing(i) + \varnothing(i-1)] \tag{22}$$

(1) The fluctuation degree of instantaneous amplitude can be reflected by the Maximum value of center normalized instantaneous amplitude spectral density $\gamma_{\max}$, whose function is to distinguish the envelope time-varying signal from the envelope constant signal, that is, to separate the MFSK signal from the MPSK signal.

$$\gamma_{max} = max|DFT(a_{cn}(i))|^2 / N_S \tag{23}$$

As shown in the Fig. 3 (a), 2FSK and 4FSK are envelope stable, 2FSK and 4FSK are equal to zero. However, 2FSK and 4FSK are small constants due to noise, while 8PSK is a constant that is not zero. Therefore, the system can be used the appropriate threshold $T5$ to divide 8PSK, 2FSK and 4FSK into 8PSK and 2FSK, 4FSK.

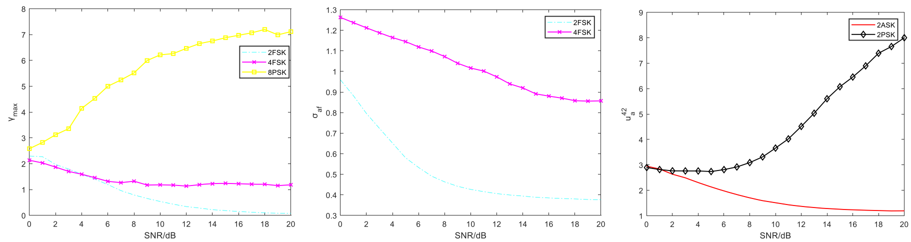

(a) $\gamma_{\max}$ for 2FSK.4 FSK.8PSK (b) σ_{af} for 2FSK.4FSK (c) u_a^{42} for 2ASK.2PSK

Fig. 3. Instantaneous characteristics of different signals

(2) The function of the Standard deviation of absolute value of zero center normalized non-weak signal instantaneous frequency σ_{af} is to distinguish the signal with absolute and direct frequency information of normalized center frequency from the signal whose absolute value is constant.

$$\sigma_{af} = \sqrt{\frac{1}{C}\left(\sum_{a_n(i) > a_i} f_N^2(i)\right) - \left(\frac{1}{C}\sum_{a_n(i) > a_i} \left|f_N^2(i)\right|\right)^2} \tag{24}$$

The absolute value of the zero center normalized instantaneous frequency of 2FSK is a constant, and its standard deviation is zero, but this system is carried out in the noisy environment, so the σ_{af} of 2FSK is a relatively small constant But 4FSK instantaneous frequency absolute value is not zero, therefore 4FSK's σ_{af} is bigger than 2FSK'S σ_{af}. As shown in the Fig. 3 (b), the system can identify 2FSK and 4FSK with appropriate threshold $T7$.

(3) Amplitude information can be represented by the Compactness of the zero-center normalized instantaneous amplitude u_a^{42}.

$$u_a^{42} = \left(E\left[f_{CN}^4(i) \right] \Big/ \left\{ E\left[f_{CN}^2(i) \right] \right\}^2 \right) - 1 \tag{25}$$

The function of u_a^{42} is to distinguish the signals with higher instantaneous amplitude distribution from those with higher instantaneous amplitude distribution. As shown in the Fig. 3 (C), there are two levels in the 2ASK, so the compactness of u_a^{42} is relatively small. The 2ASK and 2PSK are separated by appropriate threshold $T4$.

3.3 Wavelet Transform Feature

The modulated signal is transformed by wavelet. Because there are many burrs in the signal after wavelet transform, the median filter is used to remove the burrs of wavelet transform amplitude. The variance of the obtained wavelet transform amplitude after median filtering. This feature reflects the stability of wavelet transform amplitude of various signals. As shown in Fig. 4, since the amplitude stability of 64QAM signal is obviously different from that of 16QAM signal, the system uses proper threshold $T6$ to recognize the two signals in 16QAM and 64QAM

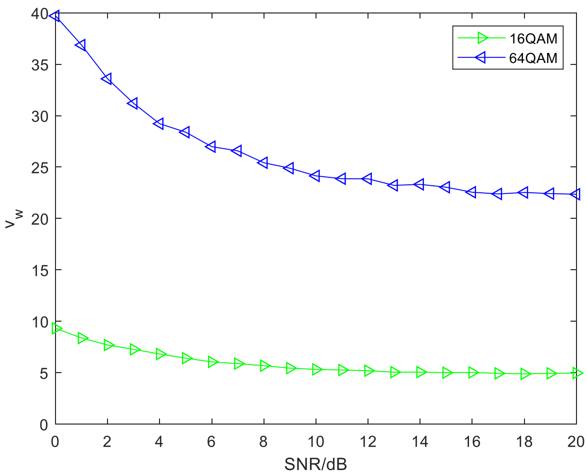

Fig. 4. V_w for 16QAM and 64QAM signals

4 Classification and Recognition of Modulation Signals Based on Decision Tree and SVM

4.1 Flow Chart

The recognition flow of the algorithm is shown in Fig. 5.

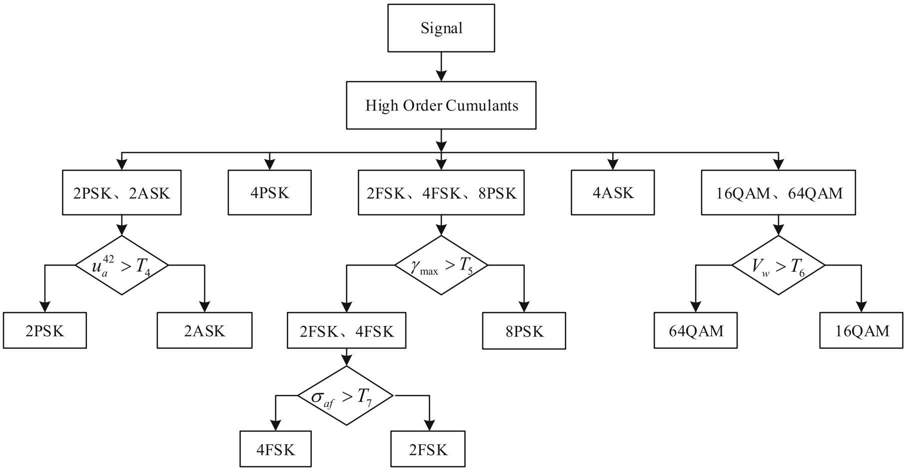

Fig. 5. Classification flowchart of modulation signals

According to the feature parameters extracted above, nine common digital signal modulation modes are identified by using binary tree structures. The 4PSK and 4ASK signals are identified, and divided into three parts:{2ASK, 2PSK}, {16QAM, 64QAM} and {8PSK, 2FSK, 4FSK}; Then{2ASK and 2PSK}, {2FSK, 4FSK, 8PSK}and{16QAM, 64QAM} are identified by u_a^{42} , γmax , V_w, and 2FSK and 4FSK are identified by σ_{af}.

4.2 Identification Simulation and Performance Analysis

In this paper, MATLAB software is used to verify the algorithm, after the down conversion to baseband signal, carrier synchronization, symbol timing, matching filter, nine common digital signal modulation mode is identified. The simulated signal is 125 symbol length, 4000 Hz carrier frequency, 16000 Hz sampling frequency, 2000 bps symbol rate, 0–20 dB signal-to-noise ratio, and the extracted characteristic parameters are averaged after 100 calculations.

Experiment 1 was a decision tree based statistical recognition model:

Figure 6 (a) is the recognition rate of 1000 times for 9 kinds of signals in 0–20 dB SNR. From Fig. 6 (a), the recognition rate of 2PSK and 2FSK is poor in 0–2 dB SNR, and most of the recognition rate is over 90% when the SNR is 5 dB. Figure 6 (b) is the total recognition rate of 9 kinds of signals under the SNR of 0 to 20 dB. From Fig. 6 (a), the overall recognition rate is below 90% under the SNR of 0 to 5 dB, and the total recognition rate is 95% and the highest is 99% under the SNR of 6 dB.

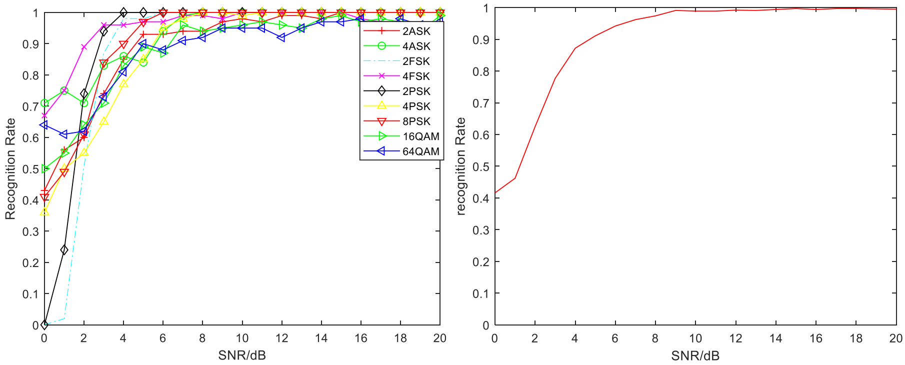

(a) (b)

Fig. 6. The recognition rate of decision tree

Experiment 2 was Support Vector Machine based recognition:

Under the condition of signal-to-noise ratio from 0 dB to 20 dB, 500 data samples are used as training set and 500 data samples are used as test set for each feature. The effect of recognition is shown in Fig. 7 (a) and Fig. 7 (b).

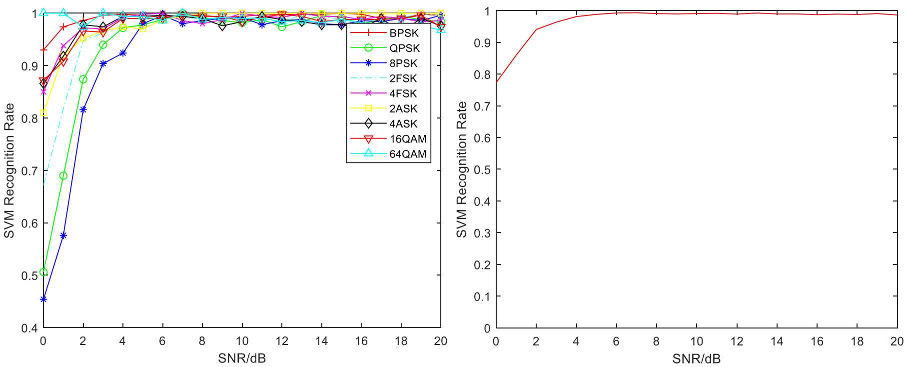

(a) (b)

Fig. 7. The recognition rate of SVM

Figure 7 (a) shows the recognition rate of 9 signals at 0–20 dB SNR. From Fig. 7 (a), the recognition rate of 4PSK and 8PSK is worse than other signals at 0–2 dB SNR, and the recognition rate of 64QAM and 2PSK signals is better at low SNR. The recognition rate of the 9 signals is over 99% when the signal-to-noise ratio is 6 dB. Figure 7.(b) is the total recognition rate of 9 kinds of signals under the signal-to-noise ratio of 0 to 20 dB. From Fig. 7 (b), the overall recognition rate is above 90% when the signal-to-noise ratio is 0 to 2 dB, and the total recognition rate is 99% when the signal-to-noise ratio is 5 dB, and the highest is 99.8%.

5 Conclusion

In this paper, the higher-order cumulants of 9 common digital signals are calculated, then the features of higher-order cumulants, 3 instantaneous features and wavelet transform are extracted, 9 kinds of signals are identified by Decision Tree Algorithm and SVM on MATLAB Platform. The experimental results show that the recognition rate of the method based on decision tree is poor at low snr. After the SNR is 6 dB, the recognition rate reaches over 90% and the highest is 99% The recognition rate of SVM method at 0 dB has reached 78%, when the SNR is 2 dB, the recognition rate is more than 90%, the recognition rate is stable at 99% when the SNR is 4 dB, and the highest recognition rate is 99.8%. Therefore, the algorithm has a good recognition rate in low SNR, which proves the effectiveness and reliability of the Algorithm.

Acknowledgements. This work has been partially supported by the National Natural Science Foundation of China project (51674109) and 2017 scientific research project of basic scientific research expenses of provincial colleges and universities in Heilongjiang Province.

References

1. Zhou, R., Liu, F., Gravelle, C.W.: Deep learning for modulation recognition: a survey with a demonstration. IEEE Access **8**, 1–12 (2019)
2. Kim, K., Polydoros, A.: Digital modulation classification: the BPSK versus QPSK case. In: MILCOM 88, Century Military Communications–What's Possible?. Conference Record. Military Communications Conference, pp. 431–436, San Diego, CA. IEEE (1988)
3. Polydoros, A., Kim, K.: On the detection and classification of quadrature digital modulations in broad-band noise. IEEE Trans. Commun. **38**(8), 1199–1211 (1990)
4. Hwang, C., Polydoros, A.: Advanced methods for digital quadrature and offset modulation classification. In: MILCOM 91- Conference Record, pp. 841–845, McLean, VA. IEEE (1991)
5. Boiteau, D., Le Martret, C.: A general maximum likelihood framework for modulation classification. In: Proceedings of the 1998 IEEE International Conference on Acoustics, Speech and Signal Processing, pp. 2165–2168, Seattle, WA. IEEE (1998)
6. Panagiotou, P., Anastasopoulos, A., Polydoros, A.: Likelihood ratio tests for modulation classification. In: MILCOM 2000 Proceedings, pp. 670–674, Los Angeles, CA. IEEE (2000)
7. Tadaion, A., Derakhtian, M., Gazor, S., Aref, M.: Likelihood ratio tests for PSK modulation classification in unknown noise environment. In: Canadian Conference on Electrical and Computer Engineering, pp. 151–154, Saskatoon, Sask. IEEE (2005)
8. Abdi, A., Dobre, O., Choudhry, R., Bar-Ness, Y., Su, W.: Modulation classification in fading channels using antenna arrays. IEEE MILCOM 2004. Military Communications Conference, pp. 211–217. IEEE, Monterey, CA (2004)
9. Li, H., Dobre, O., Bar-Ness, Y., Su, W.: Quasi-hybrid likelihood modulation classification with nonlinear carrier frequency offsets estimation using antenna arrays. In: MILCOM 2005 – 2005 IEEE Military Communications Conference, pp. 570–575, Atlantic City, NJ. IEEE (2005)
10. Xu, J.L., Su, W., Zhou, M.: Likelihood function-based modulation classification in bandwidth constrained sensor networks. 2010 International Conference on Networking. Sensing and Control (ICNSC), pp. 530–533. IEEE, Chicago, IL (2010)
11. Phukan, G.J., Bora, P.K.: Parameter estimation for blind classification of digital modulations. IET Sig. Process. **10**(7), 758–769 (2016)

12. Liu, F., Xu, J., Hu, F., Wang, C., Wu, J.: Lightweight trusted security for emergency communication networks of small groups. Tsinghua Sci. Technol. **23**(2), 195–202 (2018)
13. Arya, S., Yadav, S.S., Patra, S.K.: WSN assisted modulation detection with maximum likelihood approach, suitable for non-identical Rayleigh channels. In: 2017 International Conference on Recent Innovations in Signal processing and Embedded Systems (RISE), pp. 49–54, Bhopal, India. IEEE (2017)
14. Aslam, M.W., Zhu, Z., Nandi, A.K.: Automatic modulation classification using combination of genetic programming and KNN. IEEE Trans. Wirel. Commun. **11**(8), 2742–2750 (2012)
15. Zhang, W.: Automatic modulation classification based on statistical features and support vector machine. In: 2014 XXXI-th URSI General Assembly and Scientific Symposium (URSI GASS), pp. 1–4, Beijing, China. IEEE (2014)
16. Sun, X., Su, S., Huang, Z., Zuo, Z., Guo, X., Wei, J.: Blind modulation format identification using decision tree twin support vector machine in optical communication system. Opt. Commun. **438**, 67–77 (2019)